JOURNAL OF GUIDANCE, CONTROL, AND DYNAMICS
Vol. 19, No. 6, November–December 1996

Application of Real Structured Singular Values to Flight Control Law Validation

Piero Miotto* and James D. Paduano†
Massachusetts Institute of Technology, Cambridge, Massachusetts 02139

Flight control law validation issues raised at NASA Dryden Flight Research Center are described, and these problems are recast into the real μ analysis framework. To solve these problems, a recently developed algorithm for computing real μ is extended to include repeated real perturbations. Worst-case direction information also is provided; such information is useful in applications that require proper weighting of the perturbation block structure. An iterative weighting procedure is described that indicates the relative importance of the real uncertainties being analyzed. Other developments motivated by flight-test issues also are described: block structures for analyzing phase margin and transport delay, robustly guaranteed gain and phase margins, and implementation on simulated flight data. These tools and techniques are demonstrated on X-31 flight control laws.

I. Introduction

RECENT years have seen the steady maturation of real μ and mixed μ for multivariable robustness analysis,[1–3] as well as algorithms for computing upper and lower bounds for μ (Ref. 4). Because the definition of μ succinctly captures practically motivated robustness questions, much of the recent literature has concentrated on methods for computing tight bounds while reducing computation time.[4–8] The primary application is often considered to be design: Once algorithms are in place to reliably and efficiently compute μ, they are folded into a synthesis procedure that attempts to minimize its maximum value.[9]

The application considered here is fundamentally different. In the flight-test and control-law-validation environment, robustness characterization is an end in itself: Given a complex flight control system and nonlinear model of the flight dynamics, determine what can go wrong in flight, during maneuvers, or at the next envelope expansion point. Problems often involve delays, nonlinearities, actuator rate and/or position saturation, mode-switching pathologies, handling qualities and pilot–cockpit interactions, and complex aerodynamic/aeroelastic effects. Some of these problems are addressed by recasting them in the real μ framework.

Our approach is to describe specific questions raised during the analysis of the flight control laws for the X-31 Enhanced Fighter Maneuverability Demonstrator. Methods to answer these questions using real μ are presented. These methods form building blocks for analysis of more complex robustness questions. X-31 lateral–directional flight control laws are used to motivate the analyses and demonstrate the procedures. We address the following specific questions:

1) How should the inputs to a given Δ-block structure be weighted so that the parameters that are most important to the control system's stability are made apparent?

2) How can phase margin and transport delay be included in the robustness problem?

3) How can robustness to several aerodynamic parameters be characterized in a way that is useful to flight-test engineers?

4) How can a measure of multivariable robustness be derived during a flight test and presented in the control room?

These problems constitute only a narrow subset of the issues faced during flight-test and control-law validation. However, they are important application issues with both tutorial and practical value.

Received June 13, 1995; revision received July 9, 1996, accepted for publication July 30, 1996.

*Research Assistant, Department of Aeronautics and Astronautics, MIT Room 35-223, 77 Massachusetts Avenue.

†Associate Professor, Department of Aeronautics and Astronautics, MIT Room 35-223, 77 Massachusetts Avenue. Member AIAA.

The paper is organized as follows. The definition of the robustness problem is given first, and Dailey's algorithm for computing real μ is described and extended to the repeated real case. Then, the issue of weighting is discussed, and an example is used to highlight the importance of iterative weighting for detailed robustness analysis. Next, block structures are developed that allow phase and delay to be included as part of the real μ problem. These block structures become part of a second example, where we use the concept of robustly guaranteed gain and phase margins as a bridge between classic robustness measures and the modern techniques used here. Finally, we briefly show how an experimentally derived μ plot might be useful as part of flight-test envelope expansion procedures.

II. Notation and Definitions

The notation used in this paper is standard: superscript star $(*)$ denotes the complex conjugate transpose of a complex matrix M, a $k \times k$ identity matrix is denoted I_k, and the largest singular value of a matrix is denoted by $\bar{\sigma}(M)$.

The first step in a real μ analysis is to transform the problem into the interconnection structure of Fig. 1a, in which $M(j\omega)$ represents the nominal closed-loop dynamics and all perturbations are captured in the structured uncertainty Δ. The underlying block structure of the uncertainties in Δ is defined as follows: At each frequency ω, we have the matrix $M(j\omega) \in C^{n\times n}$. An integer $m_r \leq n$ specifies the number of real uncertainty blocks in Δ. The block structure $K(m_r)$ is a set of positive integers

$$K = \left(k_1, k_2, \ldots, k_{m_r}\right)$$

that specifies the dimensions of the perturbation blocks (these dimensions must sum to n for compatibility with M). The set of all allowable perturbations then is defined as

$$X_K = \left\{\Delta\colon \Delta = \text{block diag}\left(\delta_1 I_{k_1}, \delta_2 I_{k_2}, \ldots, \delta_{m_r} I_{k_{m_r}}\right), \quad \delta_i \in R\right\}$$

The size of the smallest destabilizing perturbation in X_K is characterized by calculating $\mu_K(M)$ at each frequency, where $\mu_K(M)$ is defined below.

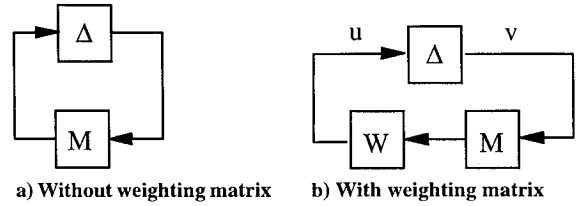

a) Without weighting matrix b) With weighting matrix

Fig. 1 Standard robustness problem.

Definition 1. The structured singular value $\mu_K(M)$ of a matrix $M \in C^{n\times n}$ with respect to a block structure $K(m_r)$ is defined as

$$\mu_K(M) = \left\{ \min_{\Delta \in X_K} [\bar{\sigma}(\Delta) : \det(I - \Delta M) = 0] \right\}^{-1}$$

with $\mu_K(M) = 0$ if no $\Delta \in X_K$ solves $\det(I - \Delta M) = 0$.

The preceding definition, if applied to our set of allowable perturbations X_K, can be simplified. In this case the 2-norm $\|\Delta\| = \sigma(\Delta)$ is identical to the norm

$$\max_i |\delta_i|$$

which is more easily interpreted in applications. Because the size of Δ is often of interest, it will be convenient to define $k_\mu \equiv \mu_K^{-1}$. Thus the size of the smallest Δ (where size is defined in terms of the preceding norms) that destabilizes the system in Fig. 1a is, by definition, k_μ. The next statements follow in a straightforward manner:

1) The system in Fig. 1a is stable for all Δ in X_K such that

$$\max_i |\delta_i| < k_\mu$$

This inequality defines a hypercube of perturbations for which the system is guaranteed to remain stable.

2) If a weighting matrix $W(j\omega)$ is introduced as in Fig. 1b, the resulting system is stable for all $\Delta \in X_K$ with $\|\Delta\| < 1$ if and only if

$$\mu_K[W(j\omega)M(j\omega)] < 1 \qquad \text{for} \qquad \omega \in (0, \infty)$$

3) If W is a diagonal frequency-independent weighting matrix,

$$W = \text{block diag}\left(w_1 I_{k_1}, w_2 I_{k_2}, \ldots, w_{m_r} I_{k_{m_r}}\right)$$

then the system in Fig. 1b is stable for Δ in X_K such that

$$\max_{i=1\cdots m_r} \left| \frac{\delta_i}{w_i} \right| < k_\mu$$

This inequality defines an elongated hypercube of guaranteed stable perturbations.

III. Stability Robustness Analysis with Iterative Weighting

A. Algorithm for Computing Real μ

Several algorithms have been proposed for the calculation of upper and lower bounds of μ; we adopt the approach outlined by Dailey.[10] Although this algorithm is not as efficient and general as other approaches,[4,6,8] it provides valuable insights into the robustness scenario, which we translate into procedures for iterative weighting.

The main assumption that is made in this algorithm is that the worst-case perturbation at a given frequency, the size of which determines μ, is in the vicinity of one of the corners of the largest stable hypercube in the uncertain parameter space. What we mean by vicinity is that all but two elements of the worst-case Δ are equal to $1/\mu$; the remaining two elements are less than or equal to $1/\mu$. Our experience with this procedure has supported the validity of this assumption, especially in the frequency region where μ is maximum. (In our experience the distance between the upper bound computed using Young's approach[4,11] and the lower bound computed using Dailey's approach is less than 10%. See Sec. IV.B for an example.) Dailey gives a full description of the algorithm; here, we will point out its main characteristics, to motivate our use of weightings. We first describe the case of distinct real uncertainties, which is Dailey's case. We then extend the analysis to include repeated real uncertainties.

1. *Distinct Real Uncertainties*

In this case all uncertain elements have multiplicity 1. The set of allowable perturbations is then defined as

$$X_K = \left\{\Delta : \Delta = \text{diag}\left(\delta_1, \delta_2, \ldots, \delta_{m_r}\right), \quad \delta_i \in R\right\}$$

To direct our search in the region of each of the corners of the hypercube, we fix all but two elements of the Δ block at initial values of $\pm k_g$. (All combinations of the sign of each element must be checked.) The values of the remaining two elements, which we designate δ_1 and δ_2, can be computed by solving a quadratic equation.[10]

If δ_1 and δ_2 are complex, or if their norm is greater than k_g, then no solution exists with $\|\Delta\| = k_g$; we therefore increase k_g and repeat. On the other hand, if the norm of (δ_1, δ_2) is smaller than k_g, then a solution with $\|\Delta\| = k_g$ does exist; in this case, we decrease k_g and repeat. The search thus converges toward the minimum value of k_g for which a solution exists with $\|\Delta\| = k_g$, and this gives us a lower bound on μ:

$$\mu_K = k_\mu^{-1} \geq \max\left(k_g^{-1}\right)$$

This search is repeated for all combinations of "all but two elements fixed," and the maximum lower bound obtained is, in practice, an excellent lower bound on μ_K. Because of the combinatorial nature of the procedure [the number of searches conducted is $m_r(m_r - 1)^{2n-3}$], practical use of the algorithm currently is limited to a maximum of about nine uncertainties.

Normally, this procedure is applied to a transfer function matrix $M(j\omega)$ over a range of frequencies. At most frequencies, the norm of (δ_1, δ_2) converges to the tightest lower bound during the first search, because one simply chooses to search in the direction that worked at the previous frequency. The remaining searches are then unnecessary; as soon as the minimum value of k_g is found, one simply verifies that there are no other directions for which a solution exists with $\|\Delta\| = k_g$. Only when a solution actually exists in a separate direction does one switch faces and iterate in the new direction.

The main advantage of this algorithm is that together with the value of μ we also know which single uncertain element is actually causing the minimum k_g. This information is particularly valuable when we want to weight the variables to find the most voluminous stable hypercube. A weighting procedure based on this information is described in Sec. III.B.

2. *Repeated Real Uncertainties*

The k_g search (in the vicinity of each corner) required in the case of a repeated real block structure is more complicated than the one described. In this case, we still fix all but two elements and perform a search, but the solution for a given k_g is not given by a simple quadratic equation. Instead, a subsearch for the (δ_1, δ_2) with minimum norm must be conducted for each value of k_g. Otherwise the procedure is unchanged.

Let us describe the subsearch. Suppose that the current direction of our search is defined by a diagonal $n_D \times n_D$ matrix D with diagonal elements equal to $+1$ or -1 defining the direction of the search. The remaining two uncertainties form a two-block structure of diagonal uncertainties whose multiplicities are k_1 and k_2:

$$\Delta' = \begin{bmatrix} I_{k_1}\delta_1 & 0 \\ 0 & I_{k_2}\delta_2 \end{bmatrix}, \qquad n_{\Delta'} = k_1 + k_2$$

We are looking for the minimum norm Δ' such that

$$\det\left\{ I - \begin{bmatrix} \Delta' & 0 \\ 0 & k_g D \end{bmatrix} \begin{bmatrix} M_{11} & M_{12} \\ M_{21} & M_{22} \end{bmatrix} \right\} = 0$$

where k_g is the current estimate of k_μ and M has been suitably partitioned. Rearranging this determinant,

$$\det\left\{ I - \begin{bmatrix} \Delta' & 0 \\ 0 & k_g I_{n_D} \end{bmatrix} \begin{bmatrix} I_{n_{\Delta'}} & 0 \\ 0 & D \end{bmatrix} \begin{bmatrix} M_{11} & M_{12} \\ M_{21} & M_{22} \end{bmatrix} \right\} = 0$$

we have

$$\det\begin{bmatrix} I_{n_{\Delta'}} - \Delta' Q_{11} & -\Delta' Q_{12} \\ -k_g Q_{21} & I_{n_D} - k_g Q_{22} \end{bmatrix} = 0$$

where the definitions of Q_{ij} are obvious. Because $\det[I_{n_D} - k_g Q_{22}]$ is different from zero except under pathological circumstances, the matrix inversion lemma allows us to convert the preceding condition to

$$\det\left[I_{n_{\Delta'}} - \Delta' Q_{11} - \Delta' Q_{12}\left(I_{n_D} - k_g Q_{22}\right)^{-1} k_g Q_{21} \right] = 0$$

Now, if we let

$$P(k_g) = Q_{11} + Q_{12}\left(I_{n_D} - k_g Q_{22}\right)^{-1} k_g Q_{21}$$

and also partition P appropriately, we can write

$$\det\left\{I_{n_{\Delta'}} - \begin{bmatrix} I_{k_1}\delta_1 & 0 \\ 0 & I_{k_2}\delta_2 \end{bmatrix}\begin{bmatrix} P_{11} & P_{12} \\ P_{21} & P_{22} \end{bmatrix}\right\} = 0$$

The condition to be met with minimum norm of (δ_1, δ_2) is then

$$\det\begin{bmatrix} I_{n_1} - \delta_1 P_{11} & -\delta_1 P_{12} \\ -\delta_2 P_{21} & I_{n_2} - \delta_2 P_{22} \end{bmatrix} = 0$$

Again, we apply the matrix inversion lemma, which gives

$$\det\left[I_{n_1} - \delta_1 P_{11}\right]$$

$$\times \det\left\{I_{n_2} - \delta_2\left[P_{22} + P_{21}\left(I_{n_1} - \delta_1 P_{11}\right)^{-1}\delta_1 P_{12}\right]\right\} = 0$$

As before, $\det[I_{n_1} - \delta_1 P_{11}]$ is not equal to zero, so we have the following result: Given a value for k_g and a guess at the size of δ_1, the value of δ_2 that makes $\det(I - \Delta M) = 0$ is given by

$$\delta_2 = \min_{\lambda_i \in R}\left|\frac{1}{\lambda_i\{B(\delta_1, k_g)\}}\right|$$

where

$$B(\delta_1, k_g) = P_{22} + P_{21}\left(I_{n_1} - \delta_1 P_{11}\right)^{-1}\delta_1 P_{12}$$

Here we have used the fact that

$$\det\left(I_{n_B} - \delta_2 B\right) = \prod_{i=1}^{n_B}[1 - \delta_2\lambda_i\{B\}]$$

where $n_B = k_1 + n_D$. Clearly, the minimum δ_2 to perturb the determinant to zero is determined by the maximum real eigenvalue of $B(\delta_1, k_g)$—the subsearch for the value of δ_1 that minimizes $\max(|\delta_1|, |\delta_2|)$ thus can be conducted.

B. Iterative Weighting Procedure

When analyzing several uncertainties in an engineering environment, it is of tremendous interest to determine which uncertain elements dominate the robustness measure, which elements are interrelated, and which elements do not greatly affect the stability of the system. Weightings are one way to address these questions. Figure 2 illustrates why weightings are important. In this simple example the stability of the system is less sensitive to uncertainty in δ_1. However, with equal weighting on these two parameters, μ analysis will not uncover this fact without additional analysis of subblocks. From Fig. 2, we can see how reweighting the parameters in the Δ block using a real diagonal weighting matrix W helps to improve our knowledge of the stable space. As the relative weighting on δ_2 goes down, the guaranteed box becomes elongated in the δ_1 direction. In the two-dimensional case, this continues until the corner of the box strikes the stability boundary; in multidimensional cases, a different edge of the stable hypercube usually strikes the boundary; weighting on the new edge is then necessary. Thus, reweighting gives a more complete picture of the robustness interrelationships. Reweighting also, in general, enlarges the guaranteed stable region, because the union of any two guaranteed regions is also guaranteed stable.

In the preceding section, we described an algorithm for calculating a lower bound of μ that is based on determining the specific uncertain element that is actually causing the maximum μ. It is reasonable then to argue that by reducing the weighting on this element we will allow larger stability bounds on the other elements, just as in our 2 × 2 example.

Let us say that we start with a certain weighting matrix:

$$W_0 = \text{diag}(1, 1, 1, 1, 1, 1)$$

After running the algorithm we find a certain value of the structured singular value μ_0. We then know that stability is guaranteed in the following n-dimensional box:

$$S_0 = \left\{\delta_i : \max_{i=1\cdots m_r}|\delta_i| < \frac{w_{0i}}{\mu_0}\right\}$$

We also know, based on the parameters that the algorithm must iterate, that the element causing the maximum μ is, for example, the one related to $W_0(2, 2)$. For the next weighting matrix we choose

$$W_1 = \text{diag}(1, 0.75, 1, 1, 1, 1)$$

We then solve for μ_1. The associated guaranteed stable region is

$$S_1 = \left\{\delta_i : \max_{i=1\cdots m_r}|\delta_i| < \frac{w_{1i}}{\mu_1}\right\}$$

In many cases, $\mu_1 < \mu_0$, and the new guaranteed stable region is more voluminous.

The stability boundaries on all of the elements other than $\Delta(2, 2)$ are larger than before. The bound on $\Delta(2, 2)$ is tighter than before, because we reduced the weighting on this element.

As we continue changing weights, the elements that never strike the stability boundary represent uncertainties that tend not to affect the stability of the system. At the end of this process, the overall guaranteed stable region is

$$S = (S_0 \cup S_1 \cup S_2 \cdots)$$

From Fig. 2, we can see how the union of all of the stability regions can provide extra information about the shape of the stability boundary. In the following example we show how, after only five reweightings, we gain a good deal of information about the robustness picture.

C. Example 1: Iterative Weighting to Isolate Important Lateral–Directional Aerodynamic Parameters of the X-31

In this example we use iterative weighting to determine the relative importance of several lateral–directional aerodynamic parameters to the robustness of a linearized X-31 lateral–directional control system. Figure 3 is a block diagram of the control system; for this example we analyze a trimmed level flight condition at a Mach number of 0.6 and altitude of 20,000 ft, 70% quasitailless. (See Sec. IV.A for a description of the quasitailless configuration; here, our purpose is not to study taillessness but to demonstrate the iterative weighting procedure.)

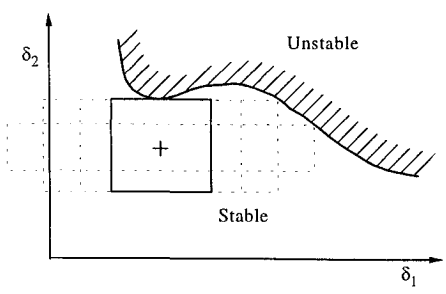

Fig. 2 Effect of weighting on guaranteed stable region.

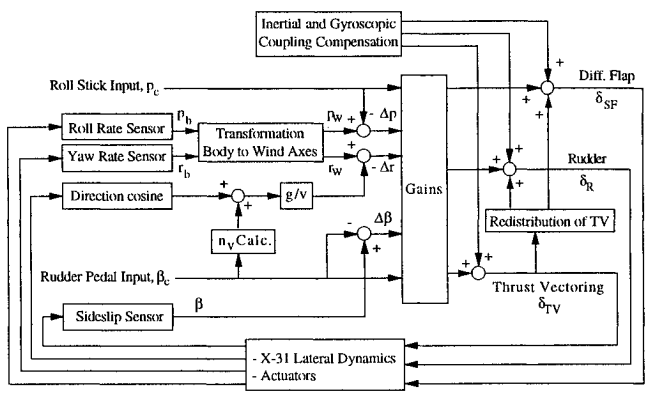

Fig. 3 X-31 lateral–directional flight control law.

Table 1 Percent allowable variations in aerodynamic elements of the control system in Fig. 3[a]

Weighting	$\Delta A(1,1)$	$\Delta A(1,2)$	$\Delta A(1,3)$	$\Delta A(2,1)$	$\Delta A(2,2)$	$\Delta A(2,3)$
Identity	44.30*[b]	44.30	44.30	44.30	44.30	44.30
$W(1,1)=0.6$	32.67*	49.02	49.02	49.02	49.02	49.02
$W(1,1)=0.36$	23.42	52.70	52.70*	52.70	52.70	52.70
$W(1,1)=0.36$, $W(3,3)=0.6$	27.21	61.24	40.83*	61.24	61.24	61.24
$W(1,1)=0.36$, $W(3,3)=0.36$	30.60*	68.86	30.60	68.86	68.86	68.86
$W(1,1)=0.216$, $W(3,3)=0.36$	21.81*	73.61	32.71	73.61	73.61	73.61

[a]Each row defines a stable hypercube of perturbations associated with the weighting at left; the union of these hypercubes is also guaranteed stable.
[b]Asterisk indicates the edge of the hypercube that is striking the true stability boundary (see Fig. 2).

The following are the elements of the A matrix that have been chosen as uncertain. Each element can be related to two aerodynamic derivatives; the first element in parentheses is the aerodynamic derivative that most strongly affects the corresponding element in A:

$$A(1,1) \Rightarrow f(C_{Lp}, C_{Np}) \qquad A(2,2) \Rightarrow f(C_{Nr}, C_{Lr})$$

$$A(1,2) \Rightarrow f(C_{Lr}, C_{Nr}) \qquad A(2,3) \Rightarrow f(C_{N\beta}, C_{L\beta})$$

$$A(1,3) \Rightarrow f(C_{L\beta}, C_{N\beta}) \qquad A(3,3) \Rightarrow f(C_{Y\beta})$$

The technique of Morton and McAfoos[12] was used to create a Δ-block corresponding to these perturbations. The initial weighting is chosen so that 100% variations in each element are given equal weighting; then the weighting procedure in Sec. III.B is applied. Table 1 lists the combined percent uncertainty that is admissible in each of the matrix elements. Note that the initial weighting allows equal-magnitude percentage perturbations in all elements. Also note that each solution of the weighted real μ problem (each row) carries with it a flag (denoted by an asterisk in Table 1) that indicates the element of the Δ block that is responsible for the bound. The subsequent μ solution (next row) is computed with the starred element from the previous solution reweighted as shown in the left-hand column. (All weightings are set to one unless noted.) The allowable perturbation on the weighted element is thus reduced, allowing the less important parameters to vary over larger percentages.

After a series of weightings are applied, the algorithm concludes that the two most important elements (in terms of the multivariable stability of the overall system) are the $A(1,1)$ element and the $A(1,3)$ element: If these elements are known within 30% accuracy, then all of the other aerodynamics need only be known to an accuracy of about 70% (fifth row of Table 1). Physically, these most important elements correspond to C_{Lp} and $C_{L\beta}$, both of which have a strong influence on the spiral stability of the aircraft. Throughout the analysis, the frequency corresponding to maximum μ is zero when $A(1,1)$ is the starred element. This frequency corresponds to a real pole, the spiral mode, violating the stability requirement. (Because the spiral mode is unstable even for the nominal system, the Level 1 handling-qualities requirement[13] for the maximum allowable unstable time constant for the spiral mode is used to analyze robustness at zero frequency. This corresponds to an indented contour along which the robustness theory is applied. For more detail see Ref. 14.) Thus the spiral-mode stability requirement sets the sensitivity of this particular system.

IV. Phase and Delay as Real Uncertainties

The algorithm and weighting procedure described is applicable to the general class of problems described in Sec. II. In applications, however, an interesting step is often that of creating the Δ-block structure to be analyzed, based on commonly asked engineering questions. For instance, classic measures of robustness (gain margin and phase margin) are still common tools for assessing the stability of flight control systems. Although singular values and structured singular values are more general measures of robustness, their interpretation is sometimes difficult; the intuition that engineers have developed for phase and gain margins is still valuable. Furthermore, the concept of delay margin is a very important variant on phase margin—transport delays are often a primary concern during flight system development, because they can change as the flight code grows.[15,16] For these reasons, we would like to be able to incorporate gain changes, phase changes, and delays into our toolbox of available perturbations to the flight system. After describing block structures for these types of perturbations, a useful way to present the resulting analysis for engineering interpretation is presented in Sec. IV.A.

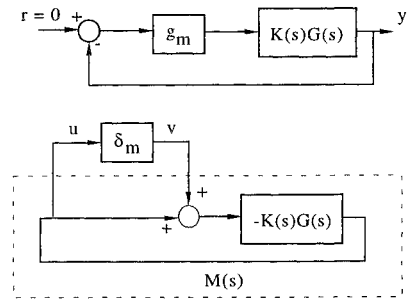

Fig. 4 Gain margin g_m and gain uncertainty δ_m.

Gain margin. It is straightforward to incorporate gain-margin concepts into a robustness problem. The interconnection of Fig. 4 shows how we have chosen to do this using a multiplicative uncertainty in the feedback path. If the uncertain gain δ_m is the only uncertainty in the system, then the single-loop gain margin is computed as $g_m = 1 + \delta_m$.

Time delay. Although a direct relationship exists between gain margin and a real uncertainty, no such relationship exists for time delay. Instead, we use an nth-order Padé approximation of a delay, and thus break out the magnitude of the delay as a real uncertainty. We know that the Laplace transform of a pure delay τ is

$$L\{f(t-\tau)\} = e^{-\tau s}F(s)$$

An nth-order Padé approximation provides a way to incorporate delay (or phase change at a specific frequency) without subsequently changing the gain of the system:

$$e^{-\tau s} = \frac{1 - p_1\tau s + p_2(\tau s)^2 \cdots p_n(\tau s)^n}{1 + p_1\tau s + p_2(\tau s)^2 \cdots p_n(\tau s)^n}$$

To incorporate τ into a real μ perturbation structure, we start with a first-order Padé and then do some block-diagram manipulations to isolate τ from the rest of the block diagram. These manipulations are shown in Fig. 5, and the resulting block diagram can be incorporated easily into, for instance, a Simulink representation of the flight system [$s = j\omega$ in the upper path of Fig. 5b is incorporated into $M(j\omega)$ during analysis].

Phase margin. To create a phase-margin block diagram, we simply realize that the phase lag introduced by the Padé approximation

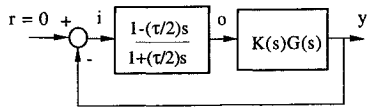

a) First-order Padé approximation

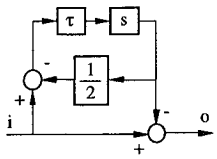

b) Padé block rearranged to isolate τ

Fig. 5 Block diagram manipulation to incorporate delay as a real uncertainty.

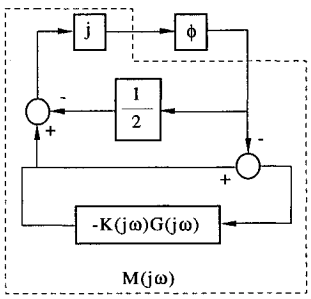

Fig. 6 Robustness problem for phase margin (first-order Padé approximation).

is a function of frequency. So, to incorporate a pure phase lag that is independent of frequency, we need a frequency-dependent time delay $\exp[-\tau(\omega)s]$, where $\tau(\omega)s = j\phi$. This results in the block diagram in Fig. 6.

Higher-order approximation of phase shift. In many applications, a first-order Padé may not adequately describe the delay or phase uncertainty. For instance, in cases where more than 90 deg of phase lag is introduced by a time delay in the frequency range of interest, the first-order Padé approximation will not be adequate, because the maximum phase lag it can introduce is 90 deg. It is also well known that the accuracy of the Padé approximation improves with its order. A second-order or higher-order Padé approximation may be translated into a real μ problem using an approach similar to that described earlier. For example, for a second-order Padé, we have

$$e^{-\tau s} \cong \frac{1-(\tau/2)s+(\tau^2/12)s^2}{1+(\tau/2)s+(\tau^2/12)s^2}$$

$$= 1 + \frac{k_1\tau s}{\tau s - a_1} + \frac{k_1^*\tau s}{\tau s - a_1^*}$$

$$k_1 = i6/\sqrt{3} \qquad a_1 = -3 + i\sqrt{3}$$

In this case the phase uncertainty in the robustness problem takes the form of a pair of repeated real uncertainties. Figure 7a shows the block diagram that describes the second-order Padé phase uncertainty. The matrices T and Q are

$$T = \begin{bmatrix} \tau s & 0 \\ 0 & \tau s \end{bmatrix} \qquad Q = \begin{bmatrix} 1/a_1 & 0 & -k_1/a_1 \\ 0 & 1/a_1^* & -k_1^*/a_1^* \\ 1 & 1 & 1 \end{bmatrix}$$

The block diagram of Fig. 7b is in the form of a standard repeated real stability robustness problem. As before, we have converted from delay to phase uncertainty by letting $\tau s = j\phi$ and incorporating j into $M(j\omega)$.

Once gain and phase perturbations can be incorporated into a system block diagram and manipulated into the standard Δ-block form, one can look at simultaneous guaranteed gain and phase margin variations for multiloop systems using real μ. By separating gain and phase into separate real perturbations, several advantages over complex uncertainties are gained: First, one can scale gain and phase separately to reflect the relative importance of each. Also, using the

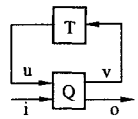

a) Second-order Padé phase uncertainty

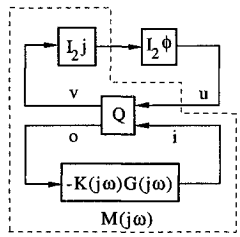

b) Standard repeated-real stability robustness problem

Fig. 7 Robustness problem for phase margin (second-order Padé approximation).

algorithm described in Sec. III, it is possible to consider only gain and phase variations in directions that are considered important. For instance, if one is primarily interested in the effects of phase lag, then phase lead perturbations can be excluded from the μ-search of Sec. III.A. Another advantage of the block structures presented here is that time-delay robustness and delay margin can now also be analyzed directly and unconservatively (see Ref. 16 for a related approach). Finally, specific robustness questions can be answered directly in terms of standard engineering measures; this is the topic of example 2.

A. Example 2: Robustly Guaranteed Phase Margins

In this section, we utilize the phase-margin block structure introduced in the preceding section and introduce the concept of a robustly guaranteed margin, which is simply a phase margin or gain margin that is guaranteed to hold in the face of other plant parameter variations. An X-31 quasitailless example illustrates the concept.

A recent flight program at NASA Dryden Flight Research Center was the X-31 quasitailless configuration, in which the rudder channel was redesigned to simulate removal of the vertical tail. Flying the X-31 without a vertical tail is possible because of the thrust-vectoring available on the aircraft; the benefits incurred (in drag, radar cross section, and high-angle-of-attack maneuverability) by removing the tail make it an attractive option to pursue. The quasitailless configuration is a conservative approach to testing the performance without the tail, because the tail can be brought back at any time, by switching back to the already-validated flight control laws. Additionally, one can phase in taillessness incrementally, using changes in the control laws instead of hardware, and fly the aircraft with, for instance, 25, 50, 75, or 100% of the tail removed. These quasitailless configurations are denoted in percent quasitaillessness, where 100% quasitaillessness refers to the tail completely removed.

The aerodynamic derivatives of the X-31 will change significantly in the quasitailless configuration. The derivatives that will change the most, and thus are subject to the highest uncertainty, are those related to the size of the tail and those related to the lateral–directional control power of thrust vectoring: $C_{L\beta}$, $C_{N\beta}$, C_{Nr}, $C_{L\delta_{TV}}$, and $C_{N\delta_{TV}}$. These derivatives, in turn, factor almost directly into the state-space system matrix elements $A(1,3)$, $A(2,3)$, $A(2,2)$, $B(1,3)$, and $B(2,3)$. The question that we pose is the following: What is the phase margin in the TV channel for different percent uncertainties in the most important aerodynamics derivatives? [Using the weighting procedure described in Sec. III.B and looking at single input/single output (SISO) and multi-input/multi-output (MIMO) gain and phase margins, we have identified phase margin in the thrust vectoring channel as the most direct measure of directional stability in the quasitailless configuration (reduced rudder authority increases the importance of thrust vectoring for stability).] In other words, what phase margin can we guarantee in the presence of 30, 40, and 50% uncertainty in the derivatives listed earlier?

Figure 8 is the Simulink block diagram utilized for this example. The uncertainties in the state-space model are incorporated into the robustness problem using the method of Morton and McAfoos.[12]

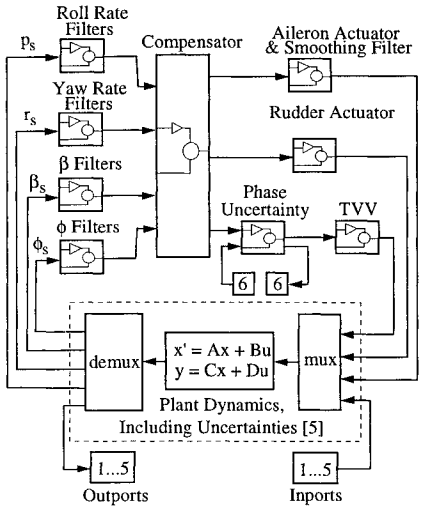

Fig. 8 Simulink setup for example 2.

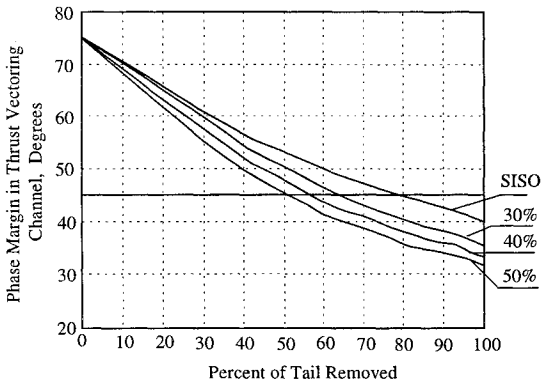

Fig. 9 Robustly guaranteed phase margin in thrust vectoring channel for various levels of uncertainty in a set of five aerodynamic coefficients (SISO corresponds to perfect knowledge of aerodynamics).

The five uncertainties in the plant and the phase uncertainty in the TV channel are apparent. Figure 9 shows the SISO and MIMO (i.e., robust) phase margins in the TV channel as functions of the percent tail reduction. This plot is constructed as follows: For each value of taillessness, the predicted aircraft dynamics are incorporated into the system structure in Fig. 8. Then the SISO phase margin is computed by letting channels 1–5 remain open. Next, the real μ analysis is performed, with channels 1–5 weighted equally (in percent). The channel 6 weighting is adjusted until the worst-case perturbation just exceeds 30%. The phase margin associated with this weighting then is considered the allowable phase margin for 30% uncertainty in all channels. The procedure then is repeated for 40 and 50% uncertainty.

As expected, the SISO phase margin is reduced from the nominal value of 75 deg to about 40 deg at 100% quasitailless. In the nominal (0% tailless) configuration, the MIMO robust and SISO phase margins are virtually the same, which means that the phase margin is not strongly affected by the size variations in the derivatives that we have chosen. As the percentage tailless increases, the MIMO robust phase margin becomes much smaller than the SISO phase margin, because the latter does not take into account plant parameter variations at all.

The conclusions one reaches from these plots are as follows: If a 45-deg phase margin is required for flight safety, the SISO phase margin suggests that one can fly to about 80% quasitailless. On the other hand, the MIMO robust phase margin indicates that, with 30% uncertainty in the uncertain elements, one should not fly above 63% quasitaillessness. With 40 and 50% uncertainty in the aerodynamic parameters, one is confident to fly only up to 57 and 51% quasitaillessness, respectively.

B. Example 3: Experimental Multivariable Gain and Phase Margins

In this example, we illustrate implementing multivariable robustness measures during flight test. We choose simultaneous phase and gain margins as an in-flight robustness measure, because these uncertainties are external to the plant dynamics and thus are analyzed more easily, and because NASA Dryden Flight Research Center currently monitors single-loop gain and phase margins in flight. Thus multivariable margins provide a smooth transition from currently used measures of system robustness. For related approaches, see Refs. 17 and 18.

Table 2 Gain and phase margin requirements for example 3

	Aileron	Rudder	TV
Gain margin, dB	3.0	0.8	3.0
Phase margin, deg	17.0	6.0	17.0

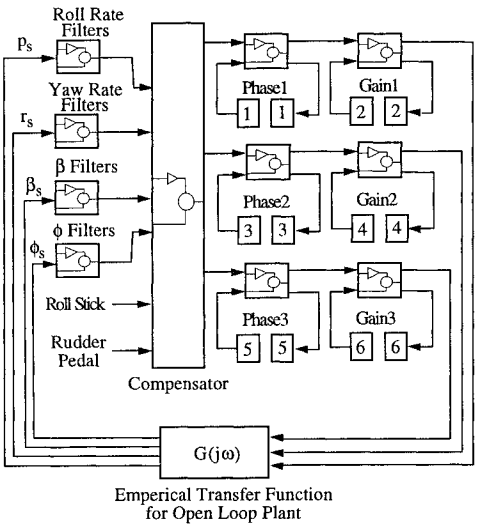

Fig. 10 Simulink block diagram for numerical experiment to determine multivariable phase and gain margins (example 3).

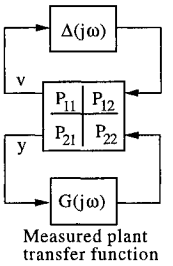

Fig. 11 Robustness problem for an experimental plant transfer function.

A Simulink block diagram of the linearized X-31 lateral–directional flight control system is presented in Fig. 10. We have inserted gain and phase uncertainties at the plant input, but any other set of uncertainties in the control systems is possible; uncertain delays, phases, and gains can be placed anywhere in the compensator block diagram. We are again analyzing the quasitailless configuration; thus we are interested in determining from flight data the robustness of the aileron and thrust vectoring channels. The requirements for gain and phase margin are defined in Table 2.

The margins on the rudder channel have been intentionally reduced because this is the channel used to destabilize the aircraft and simulate the tailless condition. The other values are reasonable combined multivariable gain and phase margins based on simulation studies. The question posed is as follows: Are the required values of gain and phase margin simultaneously guaranteed in a given actual flight condition? Figure 11 shows a block diagram of the system with the plant transfer function $G(j\omega)$, which can be identified in flight,[19] broken out. Based on this estimate, a nonparametric estimate of $M(j\omega)$ can be computed:

$$M = \left[P_{21}G(I - P_{11}G)^{-1}P_{12} + P_{22}\right]$$

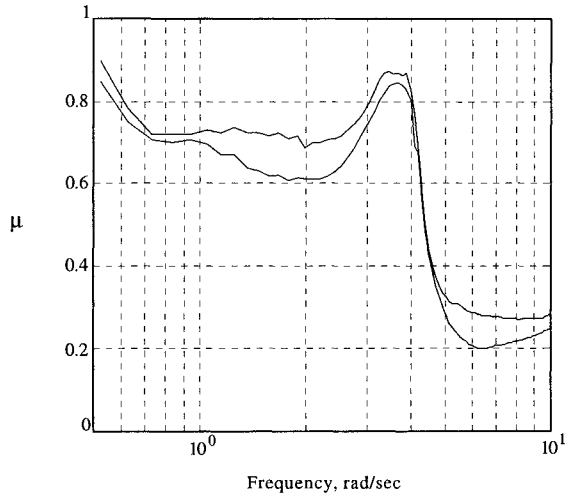

Fig. 12 Experimental robustness evaluation: real μ upper and lower bounds.

and all of the analytical procedures described in this paper can be applied.

A simple way to check robustness is through a properly weighted μ plot. If we choose the weighting such that $\|\Delta\| = 1$ corresponds to the gain and phase boundaries shown earlier, then we know from Sec. II that stability is guaranteed within the given level of uncertainty if the real μ plot is less than one. Recall that for the real diagonal uncertainty we are interested in,

$$\|\Delta\| = \max_i |\delta_i|$$

Thus if any of the weighted Δ-block parameters exceed their limits, $\|\Delta\|$ will exceed one. Figure 12 is a plot of the lower and upper bounds of the real μ calculated using an experimental $G(j\omega)$ from a nonlinear simulation.[19] Note that either the lower bound (computed by our implementation of Dailey's algorithm[10]) or the upper bound (computed using the Matlab function "mu.m"[11]) provides an excellent measure of the actual proximity of the system to the minimum robustness level, and that the flight-test engineer need only check the proximity of the plot to one to get a quick picture of the robustness situation.

From the μ plot we can see that μ is less than one. This means that the requested gain and phase margins are fulfilled in this flight condition. [The μ plot at low frequency, i.e., below 1 rad/s is not reliable because of the frequency sweep used to obtain $G(j\omega)$.] We can see that μ has a peak at about 3.5 rad/s, which is the underdamped Dutch roll mode.

V. Summary and Conclusions

We have described a set of developments that allow us to apply recent multivariable robustness analysis measures to flight-test engineering questions. The first development was the extension of Dailey's algorithm for computing real μ to include repeated real uncertainties. We also illustrated the importance of weightings and described a procedure for iteratively weighting that is tailored to sensitivity and robustness analysis, as opposed to design. In addition, we showed how to cast phase and delay uncertainty as real structured uncertainty and how to use such uncertainties in ways that provide easily interpreted information about flight safety. Finally, we demonstrated the procedures using X-31 flight control laws and how to include flight-test data into the analysis.

Clearly, useful analysis can be done using the structured singular-value framework. The examples presented here invariably corroborated previous results obtained through conventional means, which require more exhaustive approaches. More work is needed to address the plethora of flight safety, flight dynamics, implementation, and nonlinear issues that arise during flight control law validation, but the framework demonstrated here shows promise due to its versatility and intuitive appeal.

Acknowledgments

This work was supported by NASA Cooperative Agreement NCC 2-4001, John Burken, Technical Monitor. Special thanks go to John Burken, Bob Clarke, and Joe Gera for helpful discussion and to Lothar Juraschka and Pat Stoliker for technical assistance with the nonlinear simulation and Simulink modeling of the X-31.

References

[1]Young, P. M., Newlin, M. P., and Doyle, J. C., "Mu Analysis with Real Parametric Uncertainty," *Proceedings of the 30th IEEE Conference on Decision and Control* (Brighton, England, UK), Inst. of Electrical and Electronics Engineers, New York, 1991, pp. 1251–1256.

[2]Doyle, J. C., "Analysis of Feedback Systems with Structured Uncertainties," *IEE Proceedings on Control Theory and Applications*, Vol. 129, Pt. D, No. 6, 1982, pp. 242–250.

[3]Safanov, M. G., and Athans, M., "A Multiloop Generalization of the Circle Criterion for Stability Margin Analysis," *IEEE Transactions on Automatic Control*, AC-26(2), April 1981, pp. 415–422.

[4]Young, P. M., and Doyle, J. C., "Computation of μ with Real and Complex Uncertainties," *Proceedings of the 29th IEEE Conference on Decision and Control* (Honolulu, HI), Inst. of Electrical and Electronics Engineers, New York, 1990, pp.1230–1235.

[5]Sideris, A., and Sanchez Peña, R. S., "Fast Computation of the Multivariable Stability Margin for Real Interrelated Uncertain Parameters," *Proceedings of the American Control Conference* (Atlanta, GA), Inst. of Electrical and Electronics Engineers, New York, 1988, pp. 1483–1488.

[6]De Gaston, R. R. E., and Safonov, M., "Exact Calculation of the Multiloop Stability Margin," *IEEE Transactions on Automatic Control*, Vol. 33, No. 2, 1988, pp. 156–171.

[7]Fan, M. K. H., and Tits, A. L., "Characterization and Efficient Computation of the Structured Singular Value," *IEEE Transactions on Automatic Control*, Vol. AC-31, No. 8, 1986, pp. 734–743.

[8]Sanchez Pena, R. S., and Sideris, A., "A General Program to Compute the Multivariable Stability Margin for Systems with Parametric Uncertainty," *Proceedings of the American Control Conference* (Atlanta, GA), Inst. of Electrical and Electronics Engineers, New York, 1988, pp. 317–322.

[9]Doyle, J. C., "Structured Uncertainty in Control System Design," *Proceedings of the 24th IEEE Conference on Decision and Control* (Ft. Lauderdale, FL), Inst. of Electrical and Electronics Engineers, New York, 1985, pp. 260–265.

[10]Dailey, R. L., "A New Algorithm for the Real Structured Singular Value," *Proceedings of the American Control Conference* (San Diego, CA), Inst. of Electrical and Electronics Engineers, New York, 1990, pp. 3036–3040.

[11]Balas, G. J., Doyle, J. C., Glover, K., Packard, A., and Smith, R., *μ-Analysis and Synthesis Toolbox*, MuSyn, Inc., Minneapolis, MN, 1991.

[12]Morton, B. G., and McAfoos, R. M., "A μ Test for Robustness Analysis of a Real Parameter Variation Problem," *Proceedings of the American Control Conference* (Boston, MA), Inst. of Electrical and Electronics Engineers, New York, 1985, pp. 135–138.

[13]Anon., "Military Specification—Flying Qualities of Piloted Airplanes," MIL-STD MIL-F-8785C, Nov. 1980.

[14]Miotto, P., and Paduano, J. D., "Application of Real Structured Singular Values to Flight Control Law Validation Issues," AIAA Paper 95-3190, Aug. 1995.

[15]McRuer, D. T., Ashkenas, I., and Graham, D., *Aircraft Dynamics and Automatic Control*, Princeton Univ. Press, Princeton, NJ, 1973.

[16]McRuer, D. T., Myers, T. T., and Thompson, P. M., "Literal Singular-Value-Based Flight Control System Design Techniques," *Journal of Guidance, Control, and Dynamics*, Vol. 12, No. 6, 1989, pp. 913–919.

[17]Mukhopadhyay, V., and Newsom, J. R., "Application of Matrix Singular Value Properties for Evaluating Gain and Phase Margins of Multiloop Systems," AIAA Paper 82-1574, Aug. 1982.

[18]Wiseman, C. D., Hoadley, S. T., and McGraw, S. M., "On Line Analysis Capabilities Developed to Support Active Flexible Wing Wind Tunnel Tests," *Journal of Aircraft*, Vol. 32, No. 1, 1995, pp. 39–44.

[19]Burken, J. J., "Flight-Determined Stability Analysis of Multiple-Input-Multiple-Output Control Systems," NASA TM-4416, Nov. 1992.